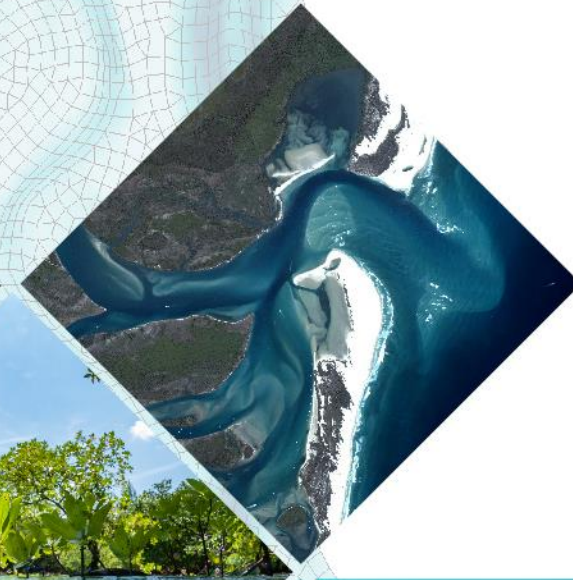
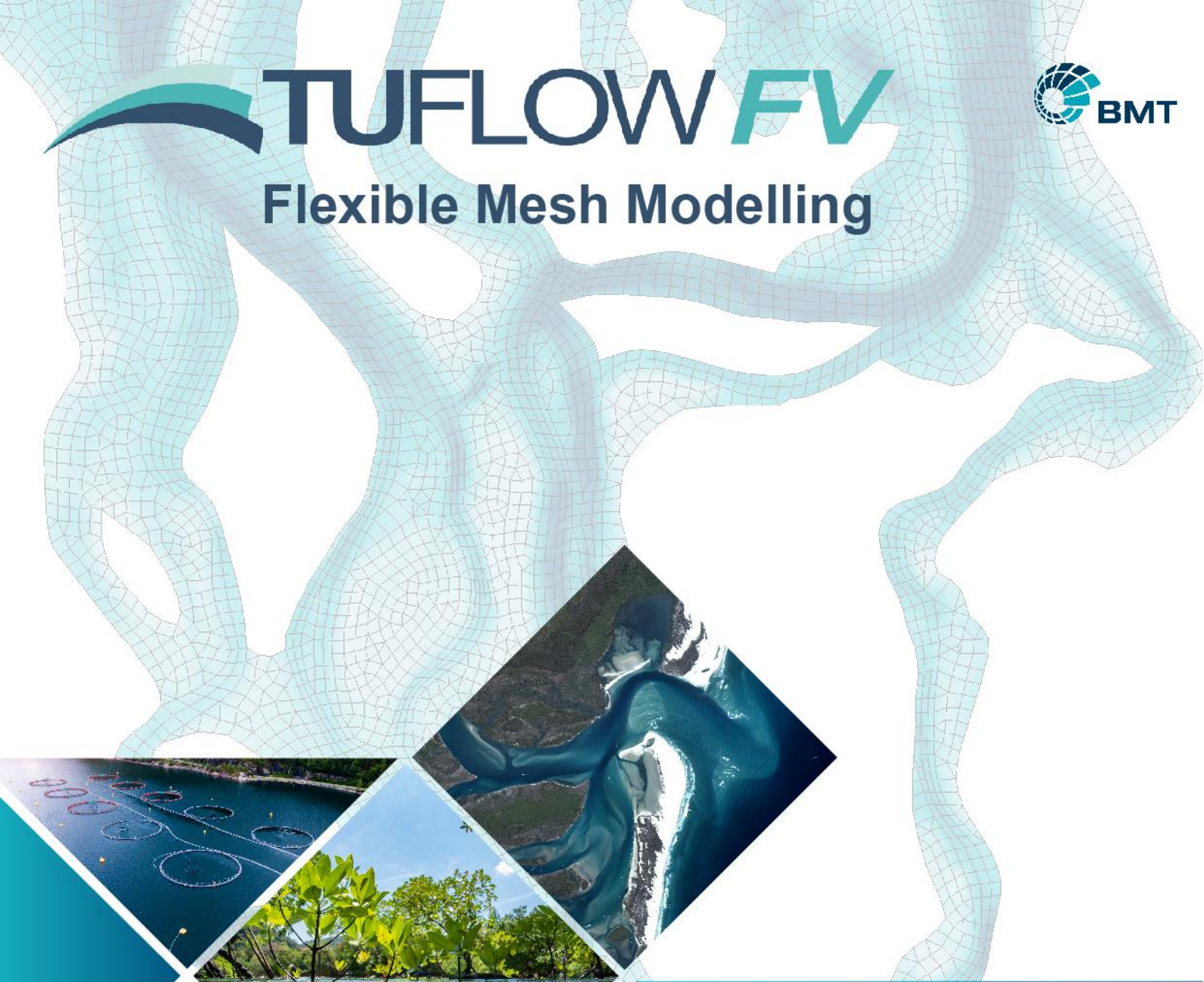




TUFLOW *FV*



Flexible Mesh Modelling



Build 2023.0

TUFLOW *FV* Science Manual

www.tuflow.com

[TUFLOW *FV* Wiki](#)

[TUFLOW Tutorial Model](#)

support@tuflow.com

Contents

1	Introduction.....	4
2	Non-Linear Shallow Water Equations (NLSWE).....	6
3	Scalar Conservation Equations	8
4	Numerical Scheme	9
4.1	Discrete System.....	9
4.2	Spatial Order.....	10
4.3	Mode Splitting	11
4.4	Flux Terms.....	12
4.4.1	Viscous Fluxes.....	12
4.4.1.1	Horizontal Viscous Fluxes	12
4.4.1.2	Vertical Viscous Fluxes.....	12
4.4.2	Inviscid Fluxes	13
4.4.2.1	Internal Mode.....	13
4.4.2.2	External Mode.....	14
4.4.2.3	Flux Correction.....	14
4.4.2.4	Scalar Inviscid Fluxes	14
4.4.3	Total Flux	14
4.4.4	Flux Spatial Integration	14
4.5	Time integration	15
4.6	Wetting and Drying	15
4.7	Source Terms	16
4.7.1	Bed slope	16
4.7.2	Coriolis	16
4.7.3	Wind Stress.....	16
4.7.4	Bed Friction.....	16
4.7.5	Surface Friction.....	17
4.7.6	Mean Sea Level and Baroclinic Pressure Gradients	18
4.7.7	Wave radiation stress	18
4.7.8	Scalar Decay.....	18
4.7.9	Scalar (Sediment) Settling.....	18
4.7.10	Other Sources/Sinks.....	18
4.8	Timestep Algorithm.....	19
5	Atmospheric Exchange	22

5.1	Shortwave Radiation.....	23
5.1.1	Shortwave Radiation Model 1	23
5.1.2	Shortwave Radiation Model 2.....	24
5.2	Longwave Radiation	27
5.2.1	Longwave Radiation Model 1	27
5.2.2	Longwave Radiation Model 2	27
5.2.3	Longwave Radiation Model 3	28
5.2.4	Longwave Radiation Model 4	29
5.2.5	Longwave Radiation Model 5	30
5.3	Latent Heat Flux	31
5.3.1	Vapour Pressures and Specific Humidities	31
5.3.1.1	Latent Heat Flux Model 1	31
5.3.1.2	Latent Heat Flux Model 2.....	33
5.3.2	Wind Transfer Coefficients	36
5.3.2.1	Wind Transfer Coefficient Model 1	36
5.3.2.2	Wind Transfer Coefficient Model 2	37
5.3.2.3	Wind Transfer Coefficient Model 3	37
5.3.3	Latent Heat Flux Calculation.....	38
5.4	Sensible Heat Flux Calculation.....	39
5.5	Total Heat Flux Calculation.....	39
6	Benchmarking.....	40
6.1	Carrier et al. 2003 Initial Value Problem.....	40
6.2	Monai Valley, Okushiri Island	42
6.3	UK Environment Agency Benchmarking Study	44
7	References	46

1 Introduction

TUFLOW FV is a numerical hydrodynamic model for the solution of the two-dimensional (2D) and three-dimensional (3D) Non-Linear Shallow Water Equations (NLSWE). The model is suitable for solving a wide range of hydrodynamic systems ranging in scale from open channels and floodplains, through estuaries to coasts and oceans.

The Finite-Volume (FV) numerical scheme employed by TUFLOW FV is capable of solving the NLSWE on both structured rectilinear grids and unstructured meshes comprised of triangular and quadrilateral elements. The flexible mesh allows for seamless boundary fitting along complex coastlines or open channels as well as accurately and efficiently representing complex bathymetries with a minimum number of computational elements. The flexible mesh capability is particularly efficient at resolving a range of scales in a single model without requiring multiple domain nesting.

Unstructured mesh geometries can be created using a suitable mesh generation tool. BMT staff generally use the SMS package (<http://www.aquaveo.com/sms>) for building meshes as well as undertaking a range of model pre-processing and post-processing tasks. Both Cartesian and Spherical mesh geometries can be used as the basis for TUFLOW FV simulations.

Three-dimensional simulations can be performed within TUFLOW FV using either sigma-coordinate or a hybrid z-coordinate vertical mesh. Three-dimensional simulations can optionally use a mode-splitting approach to efficiently solve the external (free-surface) mode in 2D at a timestep constrained by the surface wave speed while the internal 3D mode is updated less frequently.

Advection Dispersion (AD) of multiple water-borne constituents can be solved within TUFLOW FV, either coupled with a hydrodynamic simulation, or alternatively in transport mode using a pre-calculated transport file. Simple constituent decay and settling can be accommodated in the AD solutions, or alternatively more complex sediment transport algorithms can be applied through the Sediment Transport (ST) or Water Quality (WQ) Modules.

Baroclinic pressure-gradient terms can be optionally activated to allow the hydrodynamic solution to respond to temperature, salinity and sediment induced density gradients. Atmospheric heat exchange can also be calculated given standard meteorological parameter inputs by an integrated module.

TUFLOW FV has a variety of options for simulating horizontal turbulent mixing, including the Smagorinsky scheme. Simple parametric models for vertical mixing are incorporated within TUFLOW FV and for more complicated turbulence model algorithms an interface for linking with various external turbulence models has been implemented.

Both cohesive and non-cohesive sediment transport routines can be accessed through in-built TUFLOW FV modules which handle both bed and suspended load mechanisms. Dynamic morphology updating can be optionally activated.

TUFLOW FV provides multiple of options for specifying model boundary conditions, including:

- Various open boundary conditions

- Point source inflows
- Moving point source inflows
- Spatially and temporally varied forcing e.g., wind fields, short-wave forcing

2 Non-Linear Shallow Water Equations (NLSWE)

TUFLOW FV solves the NLSWE, including viscous flux terms and various source terms on a flexible mesh comprised of triangular and quadrilateral elements.

The NLSWE is a system of equations describing the conservation of fluid mass/volume and momentum in an incompressible fluid, under the hydrostatic pressure and Boussinesq assumptions. The standard form of the NLSWE, which relates the time-derivative of the conserved variables to flux-gradient and source terms, is given below.

$$\frac{\partial \mathbf{U}}{\partial t} + \nabla \cdot \mathbf{F}(\mathbf{U}) = \mathbf{S}(\mathbf{U}) \quad (1)$$

The finite-volume schemes are derived from the conservative integral form of the NLSWE, which are obtained by integrating the standard conservation equation over a control volume, Ω .

$$\int_{\Omega} \frac{\partial \mathbf{U}}{\partial t} d\Omega + \int_{\Omega} \nabla \cdot \mathbf{F}(\mathbf{U}) d\Omega = \int_{\Omega} \mathbf{b}\mathbf{v}\mathbf{S}(\mathbf{U}) d\Omega \quad (2)$$

Gauss' theorem is used to convert the flux-gradient volume integral into a boundary-integral:

$$\frac{\partial}{\partial t} \int_{\Omega} \mathbf{b}\mathbf{v}\mathbf{U} d\Omega + \oint_{\partial\Omega} (\mathbf{F} \cdot \mathbf{n}) ds = \int_{\Omega} \mathbf{b}\mathbf{v}\mathbf{S}(\mathbf{U}) d\Omega \quad (3)$$

where $\int_{\Omega} d$ represent volume integrals and $\oint_{\partial\Omega} ds$ represents a boundary integral and \mathbf{n} is the boundary unit-normal vector.

The NLSWE conserved variables are volume (depth), x-momentum and y-momentum:

$$\mathbf{U} = \begin{bmatrix} h \\ hu \\ hv \end{bmatrix} \quad (4)$$

where h is depth, u is x-velocity and v is y-velocity.

The x, y and z components of the inviscid flux (\mathbf{F}^I) and viscous flux (\mathbf{F}^V) terms in the NLSWE are given below.

$$\begin{aligned} \mathbf{F}_x^I &= \begin{bmatrix} hu \\ hu^2 + \frac{1}{2}gh^2 \\ huv \end{bmatrix}, \mathbf{F}_x^V \approx \begin{bmatrix} 0 \\ -hK_v \frac{\partial u}{\partial x} \\ -hK_v \frac{\partial v}{\partial x} \end{bmatrix} \\ \mathbf{F}_y^I &= \begin{bmatrix} hu \\ huv \\ hv^2 + \frac{1}{2}gh^2 \end{bmatrix}, \mathbf{F}_y^V \approx \begin{bmatrix} 0 \\ -hK_v \frac{\partial u}{\partial y} \\ -hK_v \frac{\partial v}{\partial y} \end{bmatrix} \\ \mathbf{F}_z^I &= \begin{bmatrix} hw \\ hwu \\ h wv \end{bmatrix}, \mathbf{F}_z^V \approx \begin{bmatrix} 0 \\ -v_t \frac{\partial u}{\partial z} \\ -v_t \frac{\partial v}{\partial z} \end{bmatrix} \end{aligned} \quad (5)$$

Some of the various source terms to the NLSWE are provided below:

$$\mathbf{S} = \begin{bmatrix} gh \frac{\partial z_b}{\partial x} + fvh - \frac{h}{\rho_0} \frac{\partial p_a}{\partial x} - \frac{hg}{\rho_0} \int_z^0 \frac{\partial \rho}{\partial x} dz - \frac{1}{\rho_0} \left(\frac{\partial s_{xx}}{\partial x} + \frac{\partial s_{xy}}{\partial y} \right) + \frac{\tau_{sx}}{\rho_0} - \frac{\tau_{bx}}{\rho_0} \\ gh \frac{\partial z_b}{\partial y} - fuh - \frac{h}{\rho_0} \frac{\partial p_a}{\partial y} - \frac{hg}{\rho_0} \int_z^0 \frac{\partial \rho}{\partial y} dz - \frac{1}{\rho_0} \left(\frac{\partial s_{yx}}{\partial x} + \frac{\partial s_{yy}}{\partial y} \right) + \frac{\tau_{sy}}{\rho_0} - \frac{\tau_{by}}{\rho_0} \end{bmatrix} \quad (6)$$

where

- $\frac{\partial z_b}{\partial x}, \frac{\partial z_b}{\partial y}$ are the x- and y-components of bed slope
- f is the Coriolis coefficient
- ρ is the local fluid density, ρ_0 is the reference density and p_a is the mean sea level pressure
- s_{ij} is the short-wave radiation stress tensor, and
- τ_s and τ_b are respectively the surface and bottom shear stress terms (where applicable).

Other source terms not included above include inflow/outflow to/from the water column.

3 Scalar Conservation Equations

Analogous conservation equations are solved for the transport of scalar constituents in the water column.

$$U = [hC] \quad (7)$$

where C is the constituent concentration. The flux components of the scalar conservation equation are:

$$\begin{aligned} F_x^I &= [huC], \quad F_x^V \approx \left[-h \left(D_{xx} \frac{\partial C}{\partial x} + D_{xy} \frac{\partial C}{\partial y} \right) \right] \\ F_y^I &= [hvC], \quad F_y^V \approx \left[-h \left(D_{yx} \frac{\partial C}{\partial x} + D_{yy} \frac{\partial C}{\partial y} \right) \right] \\ F_z^I &= [hwC], \quad F_z^V \approx \left[-hv_t' \frac{\partial C}{\partial z} \right] \end{aligned} \quad (8)$$

The source components may include scalar decay and settling:

$$S = [-K_d hC - w_s C] \quad (9)$$

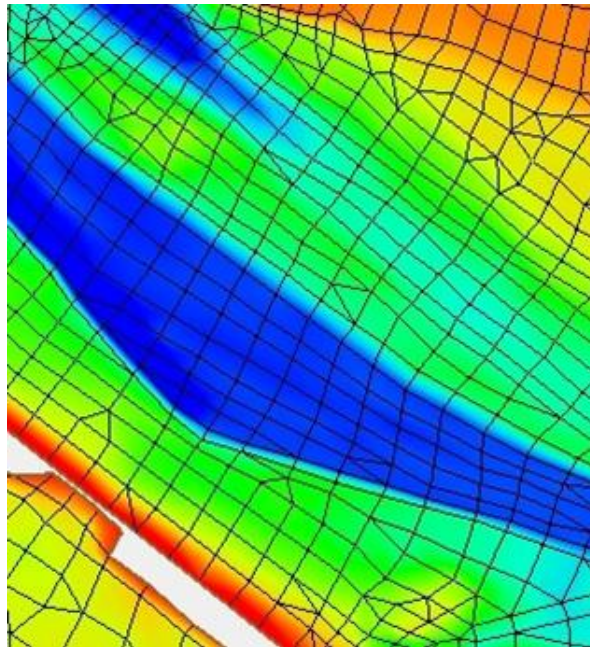
where K_d is a scalar decay-rate coefficient and w_s is a scalar settling velocity.

4 Numerical Scheme

The system of equations described above is solved using a Finite-Volume numerical scheme, as described below. Further details about Finite Volume methods for hyperbolic systems can be found in Leveque (2002).

4.1 Discrete System

The spatial domain is discretised using contiguous, non-overlapping triangular and quadrilateral cells (or elements).



A cell-centred spatial discretisation is adopted for all NLSWE conserved variables. The discrete form of the equations for cell i , with $k = 1, N_k$ cell-faces is:

$$\frac{\partial U_i}{\partial t} = -\frac{1}{A_i} \sum_{k=1}^{N_k} (\mathbf{F}_k \cdot \mathbf{n}_k) L_k + \mathcal{S}_i \quad (10)$$

In this discrete equation U_i represents the volume-average of the conserved variables in cell i , A_i is the cross-sectional (plan) area of the cell and \mathcal{S}_i is the volume-average source term/s. A first-order midpoint quadrature is used to evaluate the cell boundary flux integral, where \mathbf{n}_k is the boundary/face unit normal vector for face k and L_k is the corresponding face length. The discrete conserved variable field is assumed to be continuous within a cell but discontinuous at the cell-faces.

The finite-volume form of the conservation equation has delivered an Ordinary Differential Equation (ODE) from the original Partial Differential Equation (PDE) form of the conservation equation (Equation 1). This allows the solution of the conservation system of equations to be separated into a two-stage algorithm:

1. The spatial integration of the discrete flux and source components (RHS of Equation 10)
2. The time integration of the discrete system of system of conservation equations

4.2 Spatial Order

The first-order form of the finite volume schemes assumes a piecewise constant U_i within each model cell (Leveque, 2002). Finite-volume schemes with higher-order spatial accuracy can be derived by re-constructing a piecewise continuous $U_i(x, y, z)$ within each model cell. For instance, a second-order spatial scheme can be derived by re-construction of a piecewise linear $U_i(x, y, z)$, while a third-order spatial scheme would require re-construction of a piecewise parabolic $U_i(x, y, z)$. It should be noted that the discrete U_i remains discontinuous at cell-faces even for schemes higher than first-order (Hubbard, 1999).

The higher spatial orders can significantly reduce numerical diffusion where the physical system being solved includes large spatial gradients relative to the discrete mesh size. Numerical diffusion can also be reduced through selection of a finer mesh resolution; however the higher spatial order schemes will generally achieve this outcome with less increase in computational overhead.

In general, the solution will only benefit from higher spatial order when the spatial gradients become sufficiently large relative to the mesh size. This can only be determined by testing for improvements in the higher-order solution relative to the first-order solution. If the first-order and high-order solutions are more or less identical for the particular model purpose, then it is generally appropriate to adopt the first-order accuracy. However, if the solutions are significantly different this suggests that first-order numerical diffusion is substantial relative to the physical fluxes that are being resolved in the model. In this case the higher-order solution is probably of a higher quality, though care must be exercised with the higher order solutions to ensure that spurious “overshoots” at the cell faces are avoided by the reconstruction procedure.

The Total Variation Diminishing (TVD) property (and hence stability) of the higher-order scheme solution is achieved using a choice of gradient limiter schemes. A variety of gradient limiters are available in TUFLOW FV and are listed in Table 1-1 in order from least to most “compressive”. The most “compressive” schemes will maximise the resolution of sharp gradients but may do so at the expense of additional computational overhead. The most compressive gradient limiter schemes also increase the risk of generating spurious “overshoots” within the solution.

Within TUFLOW FV horizontal and vertical reconstructions are performed separately. A first-order horizontal reconstruction can be combined with a second-order vertical reconstruction, and vice-versa.

Table 1-1 Overview of gradient limiter schemes applied in TUFLOW FV

	Horizontal gradient limiter scheme	Vertical gradient limiter scheme
Least Compressive		MINMOD Fringer et al. (2005)
↓	Limited Central Difference (LCD) Batten et al. (1996)	Maximum Central Fringer et al. (2005)
Most Compressive	Maximum Limited Gradient (MLG) Batten et al. (1996)	Superbee Fringer et al. (2005)

4.3 Mode Splitting

Efficient integration of the NLSWE is achieved through a mode splitting scheme, whereby different components of the governing equations are updated using an appropriate timestep selected by taking into account physical and numerical convergence and stability considerations (e.g. Shchepetkin & McWilliams, 2005).

A reduced set of equations comprising all terms other than the barotropic (or free-surface) pressure-gradients is initially partially solved. As part of this solution, an appropriate “internal mode” timestep is calculated that obeys both:

- Courant-Freidrich-Levy (CFL) constraints imposed by the advective current speeds
- Peclet number (Pe) constraints imposed by the diffusion terms

Prior to updating (or time-integrating) the solution an “external mode” loop is entered, in which a 2D depth-averaged reduction of the 3D NLSWE is solved multiple times, using a timestep that obeys the barotropic Courant-Freidrich-Levy (CFL) constraint imposed by the shallow water wave speed $\bar{u} \pm \sqrt{gh}$ (where \bar{u} is the depth-averaged current speed). The external mode loop is repeated until the cumulative timestep is approximately equal to the internal mode timestep.

The depth-averaged inviscid fluxes from the external mode solution are then used to correct the internal mode inviscid fluxes so that they now represent the total inviscid flux for the 3D solution. The corrected fluxes are used to update the full 3D solution.

A stability constraint imposed by the baroclinic internal wave speed is not explicitly calculated and in some instances may not be automatically met by the mode splitting scheme. This can be addressed by the user reducing the upper-limiting timestep, where oscillations in the pycnocline are seen to be generating numerical instabilities.

Viscous fluxes and both inviscid and viscous scalar transport fluxes are calculated only for the “internal mode” (outer) loop.

Mode splitting can be disabled for 2D simulations and this configuration can be more computationally efficient for fast, shallow flow scenarios where the “internal mode” and “external mode” timesteps are similarly restrictive.

Currently, 3D simulations are only supported with mode splitting enabled.

4.4 Flux Terms

A key step in the Finite-Volume numerical scheme is the calculation of numerical fluxes across cell boundaries:

- Inviscid fluxes (F_x^I, F_y^I, F_z^I) represent the directly resolved flux of mass and momentum between adjacent cells
- Viscous fluxes (F_x^V, F_y^V, F_z^V) represent the “mixing” of mass and momentum that is not directly resolved as advection within the numerical model

4.4.1 Viscous Fluxes

Viscous flux terms are calculated using the traditional gradient-diffusion model with a variety of options available for the calculation of eddy-viscosity and scalar diffusivity.

4.4.1.1 Horizontal Viscous Fluxes

The horizontal viscous fluxes (F_x^V, F_y^V) are calculated according to Equations 5 and 8. The horizontal eddy-viscosity can be specified directly or can be calculated from the Smagorinsky formulation below.

$$K_v = c_s^2 l_s^2 \sqrt{\left(\frac{\partial u}{\partial x}\right)^2 + \left(\frac{\partial v}{\partial y}\right)^2 + \frac{1}{2}\left(\frac{\partial u}{\partial y} + \frac{\partial v}{\partial x}\right)^2} \quad (11)$$

where c_s is the Smagorinsky coefficient and l_s is the Smagorinsky lengthscale which is related to the local mesh size.

The horizontal scalar-diffusivity tensor can also be specified directly (as an isotropic constant value), can be calculated from a Smagorinsky formulation (Equation 11) or via the “Elder” formulation (Falconer et al., 2005). The Elder model calculates a non-isotropic diffusivity tensor that accounts for velocity dispersion processes not resolved in 2D depth-averaged models.

$$\begin{aligned} \mathbf{D}_{xx} &= (D_l u^2 + D_t v^2)h/u_* \\ \mathbf{D}_{yy} &= (D_l v^2 + D_t u^2)h/u_* \\ \mathbf{D}_{xy} = \mathbf{D}_{yx} &= (D_l - D_t)uvh/u_* \end{aligned} \quad (12)$$

and D_l, D_t are the Elder coefficients in the directions lateral to the local current and transverse to the local currents respectively and $u_* \left(= \sqrt{|\boldsymbol{\tau}_b|/\rho} \right)$ is the friction velocity. The observed range of values for D_l, D_t derived from measurements is discussed in Fisher et al., 1979. In 3D model simulations the Smagorinsky formulation is generally more applicable.

4.4.1.2 Vertical Viscous Fluxes

The vertical viscous fluxes F_z^V are calculated according to Equations 5 and 8. An unconditionally stable semi-implicit scheme is adopted in the discretisation of F_z^V in order to avoid these terms imposing restrictions on the model timestep.

The vertical eddy viscosity, v_t , can be directly specified, via an external turbulence scheme (such as [GOTM](#)), or may be calculated from the simple parametric model formulation including Munk & Anderson (1948) stability function:

$$v_{t0} = \kappa u_* z \left(c_1 - c_2 \frac{z}{h} \right) \quad (13)$$

$$v_t = \sqrt{1 + 10 \cdot Ri} v_{t0} \quad (14)$$

where Ri is the gradient Richardson number defined as,

$$Ri = \frac{N^2}{(\partial u / \partial z)^2} \quad (15)$$

And N is the Brunt-Vaisala frequency (or buoyancy frequency)

$$N = \sqrt{-\frac{g}{\rho} \frac{\partial \rho}{\partial z}} \quad (16)$$

The scalar diffusivities, v_t' , may also be directly specified or it may be calculated using the parametric model formulations below, which vary depending on scalar type:

Passive tracers:

$$v_t' = v_t$$

Temperature and salinity

$$v_t' = \begin{cases} \frac{1}{\sigma} v_t (1 + 3.33 Ri)^{-1.5} & Ri > 0. \\ \frac{1}{\sigma} v_t & Ri \leq 0 \end{cases} \quad (17)$$

Sediment fractions

$$v_t' = \beta v_t$$

Where σ is the neutral turbulent Prandtl number and β is the sediment mixing coefficient.

4.4.2 Inviscid Fluxes

Inviscid fluxes F_x^I, F_y^I, F_z^I represent the directly resolved flux of mass and momentum between adjacent cells. Inviscid fluxes are calculated for each cell-face based upon the conserved variable state immediately on either side of the cell-face. For the first-order spatial scheme these values are equivalent to the adjacent-cell-averages, whereas the higher-order schemes will have reconstructed the conserved variable state at the cell-faces from the cell-averages.

4.4.2.1 Internal Mode

The “internal mode” inviscid flux calculations solve the full 3D NLSWE, excluding the terms related to the free-surface pressure gradient. A centred scheme is used to evaluate the internal mode mass flux while an upwind scheme is used for the momentum flux terms. “Flux-like” source terms originating due to bed slope and from the baroclinic pressure gradients are included in the cell-face flux calculation rather than included in the volume-integrated source term in Equation 10.

The stable internal mode timestep is dictated by internal advection CFL constraints in combination with viscous flux Peclet constraints. A stable internal mode timestep is selected prior to entering the external mode.

4.4.2.2 External Mode

The “external mode” inviscid flux calculations solve the 2D depth-averaged NLSWE. For 3D simulations, the external mode is initiated by calculating depth-averages of the 3D conserved variable fields. Viscous fluxes and baroclinic pressure gradients are also depth-integrated at the start of the external mode loop.

The 2D depth-averaged NLSWE are solved using Roe’s approximate Riemann solver (Roe, 1981). “Flux-like” source terms originating due to bed slope and from the depth-averaged baroclinic pressure gradients are included in the cell-face flux calculation rather than included in the volume-integrated source term in Equation 10 (refer Section 4.7).

The stable external mode timestep is dictated by the surface gravity wave CFL constraint in combination with the depth-averaged viscous flux Peclet constraints (Murillo et al., 2005). A stable external mode timestep is selected at each external mode sub-timestep. Within the external mode loop, multiple sub-timesteps are executed prior to returning to the outer “internal mode” loop.

4.4.2.3 Flux Correction

The “internal mode” inviscid fluxes are corrected using the depth-averaged “external mode” fluxes that have been integrated in time through the external mode loop.

When mode splitting is optionally disabled, the complete NLSWE (including free-surface pressure gradients) are solved directly using the same NLSWE flux scheme described for the External Mode calculation. This option is currently only available for 2D model simulations, and can be more computationally efficient than the mode split scheme for pure hydrodynamic simulations of relatively fast shallow flows.

4.4.2.4 Scalar Inviscid Fluxes

Scalar inviscid fluxes are calculated from the product of the “corrected” mass flux and the upwind cell-face concentration. Knowing the “corrected” horizontal inviscid fluxes, the vertical inviscid fluxes are calculated from the continuity equation.

4.4.3 Total Flux

The total flux vector is the sum of the corrected inviscid and viscous flux components.

4.4.4 Flux Spatial Integration

The first term on the RHS of Equation 10 requires calculating the boundary-integral of the total flux vector normal component and is approximated using a simple midpoint quadrature rule.

The momentum flux terms are first converted to a momentum flux difference prior to the integration step. In the case of spherical coordinates, the momentum and flux vectors are shifted from a face-centred to cell-centred basis by applying a “parallel transport” transformation. This accounts for rotation of the spherical coordinates vector basis during translation on the sphere (Rossmannith, 2004).

4.5 Time integration

Both internal mode and external mode temporal integration is performed with an explicit Euler scheme. Accordingly, a stable time step must be bounded by the Courant-Friedrich-Levy (CFL) criterion for the wave propagation and advective terms and by the Peclet criterion for the diffusive terms (Murillo et al., 2005).

The external mode CFL criterion is given by

$$\frac{|\mathbf{u} \cdot \mathbf{n} \pm \sqrt{gh}| \Delta t}{L^*} \leq 1 \quad (18)$$

where Δt is the integration timestep and L^* is a cell-size dependent length scale.

The internal mode CFL criterion is given by:

$$\frac{\max(|\mathbf{u} \cdot \mathbf{n}|, c_{baro}) \Delta t}{L^*} \leq 1 \quad (19)$$

where c_{baro} is the baroclinic (internal) wave speed.

The Peclet criterion is given by:

$$\frac{|\mathbf{D} \cdot \mathbf{n}| \Delta t}{L^{*2}} \leq 1 \quad (20)$$

In the above stability criteria relationships, the cell-size dependent length-scale L^* is calculated for each cell-face as:

$$L^* = \frac{\min(A_i, A_j)}{L_k} \quad (21)$$

where A_i, A_j are the adjacent cell-areas and L_k is the face length.

A variable time step scheme is implemented to ensure that the CFL and Peclet criterion are satisfied at all points in the model with the largest possible time step. Outputs providing information relating to performance of the model with respect to the CFL criterion are provided to enable informed refinement of the model mesh in accordance with the constraints of computational time (refer TUFLOW FV user manual for details).

In stratified flows the baroclinic wave speed may impose a constraint on the stable internal mode timestep. However, the internal mode timestep is not automatically adjusted to satisfy the baroclinic wave speed limit. Additionally, the mode splitting scheme stability may benefit from limiting the ratio between the internal and external mode timestep to around 10 or less.

Maximum and minimum timestep limits are specified by the user. The maximum limit should be used to limit the upper internal mode timestep. The minimum limit should be used to restrict the external mode timestep in the event of a model instability, as it is preferable to have the model violate the prescribed stability bounds than have the timestep decrease towards zero.

4.6 Wetting and Drying

In very shallow regions ($\sim < 0.05\text{m}$ depth), the momentum terms are dropped in order to maintain stability as the NLSWE approach the zero-depth singularity. Mass conservation is maintained both

locally and globally to the limit of numerical precision across the entire numerical domain, including wetting and drying fronts. A conservative mass re-distribution scheme is used to ensure that negative depths are avoided at numerically challenging wetting and drying fronts without recourse to adjusting the time step (Brufau et al., 2004; Murillo, 2006). Regions of the model domain that are effectively dry are readily dropped from the computations.

4.7 Source Terms

4.7.1 Bed slope

Bed slope integral source terms are calculated using a face-centred “upwind flux correction” within the internal and external mode numerical flux solvers.

$$\int_{\Omega} -gh\nabla\mathbf{z}_b \partial\Omega \cong \sum_{k=1}^{N_k} \beta^*(\Delta z_b)_k L_k \quad (22)$$

That is, the cell-face bed elevation jump (Δz_b) becomes a correction term $\beta^*(\Delta z_b)$ to the cell-face numerical flux terms. This numerical approach provides consistent upwinding between flux and bed-slope source terms. This is essential to obtaining the required numerical balance between these terms, at for instance the quiescent state equilibrium. Further details are provided in the following references; Hubbard & Garcia-Navarro, 2000; Murillo, 2006.

4.7.2 Coriolis

Coriolis forces due to Earth’s rotation are calculated as cell-averaged source terms in the momentum equation. The Coriolis coefficient f_c is calculated from:

$$f_c = 2\Omega_r \quad (23)$$

where Ω_r is the angular frequency of Earth’s rotation (rad/s) and ϕ is the geographic latitude (radians).

For Cartesian coordinate system models the latitude is specified as a domain constant value. In spherical coordinate models the latitude is obtained locally from the y-coordinate value.

4.7.3 Wind Stress

The cell-averaged surface stress vector due to wind is calculated from

$$\boldsymbol{\tau}_{sw} = \rho_a c_{dw} \mathbf{u}_w |\mathbf{u}_w| \quad (24)$$

where the wind drag coefficient is calculated using the empirical formula of Wu (1980; 1982)

$$c_{dw} = \begin{cases} c_a & w_{10} < w_a \\ c_a + \frac{c_b - c_a}{w_b - w_a} (w_{10} - w_a) & w_a \leq w_{10} < w_b \\ c_b & w_{10} \geq w_b \end{cases} \quad (25)$$

with default parameters $(w_a; c_a; w_b; c_b) = (0.0; 0.8e-3; 50.0; 4.05e-03)$.

4.7.4 Bed Friction

Bed friction momentum sink terms are calculated using a quadratic drag law.

$$\tau_{bf} = \rho c_{dbu} |u| \quad (26)$$

where the bottom drag coefficient can be calculated using a roughness-length relationship:

$$c_{db} = \left(\frac{\kappa}{\ln(30.z'/k_s)} \right)^2 \quad (27)$$

The above relationship assumes a rough-turbulent logarithmic velocity profile in the lowest model layer, where κ is von Karman's constant, k_s the effective bed roughness length (equivalent Nikuradse roughness) and z' is the height of the bottom cell-centroid above the seabed.

Instead of specifying k_s a Manning's n roughness can be specified and is internally converted into an equivalent roughness length:

$$k_s = 11. h \exp\left(-\frac{\kappa h^{1/6}}{\sqrt{gn}}\right) \quad (28)$$

Bed roughness values (k_s : or Manning's n) may be specified globally or for "material" types as defined in the mesh geometry file.

The above bed friction formulations are generally applicable in both 2D (depth-averaged) and 3D configurations. In 2D situations the Manning's n formulation is equivalent to the following equation for the friction slope (Chow, 1959).

$$S_f = \frac{\tau_{bf}}{\rho gh} = \frac{n^2 \bar{u} |\bar{u}|}{h^{4/3}} \quad (29)$$

It should be noted that given the same bed-roughness parameters calculated bed friction energy losses are typically not exactly equivalent for 2D and 3D simulations except in the simplest fully-developed, uniform flow scenarios. This is because the 2D models "assume" a logarithmic velocity profile extending over full-depth, whereas 3D simulations resolve the vertical velocity profile, which may be non-logarithmic in some more complex flow situations.

Integrated bed friction source terms are calculated using a semi-implicit discretisation in order to maintain unconditional numerical stability of these terms in high-velocity or shallow flows (Brufau et al, 2004). Coupling of the internal/external modes is achieved by applying the internal mode (3D) bed friction as an explicit momentum sink/source term during external mode (2D) loop calculations.

4.7.5 Surface Friction

Surface friction (e.g. from ice or pontoon structures) can be applied using a quadratic drag law. Only a roughness length input (k_s) is supported for surface friction specification. It should be noted that the surface friction terms are calculated explicitly and therefore do not exhibit the same unconditional stability property as the bed friction terms. In some circumstances these terms may generate numerical instabilities in high-velocity or shallow flows, which can be treated with a timestep reduction. Surface roughness values may be specified globally or for "material" types as defined in the mesh geometry file.

4.7.6 Mean Sea Level and Baroclinic Pressure Gradients

Mean Sea Level Pressure and Baroclinic pressure gradient source terms are calculated as a face-centred flux correction terms within the internal and external mode numerical flux solvers. That is the pressure gradient terms are treated in a similar manner to the bed slope source terms as described in Section 4.7.1, i.e.

$$\int_{\Omega} -(\nabla P) \partial\Omega \cong \sum_{k=1}^{N_k} \eta^* (\Delta P)_k L_k \quad (30)$$

where ∇P is the gradient of the combined atmospheric and baroclinic pressure fields and η^* is a face-centred flux correction due to the cell-face pressure jump ΔP . This is analogous to converting the cell-volume source term integral into a cell-boundary source term integral using Gauss' theorem.

4.7.7 Wave radiation stress

Wave fields are applied as spatially and temporally varying datasets on a 2D rectilinear/curvilinear grid. The wave field boundary condition data is specified in a netcdf file and applied to the TUFLOW FV model as described in the user manual.

Wave radiation stress gradients are calculated as cell-centred source terms:

$$\int_{\Omega} \left(\frac{\partial s_{xx}}{\partial x} + \frac{\partial s_{xy}}{\partial y} \right) \partial\Omega \quad (31)$$

or as face-centred momentum flux source terms.

The wave radiation stress gradients are currently distributed uniformly throughout the water column. More advanced options will be implemented in future release/s of the software.

4.7.8 Scalar Decay

Tracer constituents can be specified with a linear scalar decay property (Equation 9), where K_d is the constant linear decay coefficient. Scalar decay is discretised explicitly as a cell-centred integral source term. Numerical stability of this term is not guaranteed for large K_d or for large model timesteps.

4.7.9 Scalar (Sediment) Settling

Tracer and sediment constituents can be specified with a settling velocity w_s Equation 9.

Within the water column, the settling velocity contributes an additional (vertically downward) inviscid flux component. At the seabed the settling velocity contributes a sink from the water column and source into the bed. In the case of sediment fractions the mass transferred to the bed is subsequently tracked within the TUFLOW FV Sediment Transport Module. The passive tracer constituent mass exiting the water column is no longer tracked.

4.7.10 Other Sources/Sinks

Inflows/outflows into/from model domain can be specified as boundary conditions to the model. These boundaries typically require specification of the volumetric flow rate (inflow = positive, outflow = negative) and associated scalar concentrations.

In the case of an outflow specification, either the internal domain concentration (at the extraction location) can be applied (this is the default) or alternatively the outflow concentration can be directly specified. The latter approach might be used to simulate evaporation from the water column, where there is no scalar mass loss corresponding to the volumetric loss, i.e. the outflow concentration for the scalar constituents is zero. Another option, where there is no volumetric source, is to directly specify the scalar mass fluxes.

The spatial definition of source/sink boundary conditions, includes the following options as described in the user manual:

- Global (spatially constant and variable) source/sinks
- Point source/sinks
- Moving point source/sinks

The vertical distribution of the source/sink terms can be specified as part of the boundary condition definition. A detailed description of the available source/sink boundary condition options is provided in the TUFLOW FV user manual.

The TUFLOW FV Sediment Transport Module calculates the sediment settling/mixing parameters and bed-pickup sink/source terms required as inputs and boundary conditions to the suspended sediment advection/dispersion calculations. Additionally this module can calculate bed load transport and bed-elevation update in response to sediment transport gradients.

The TUFLOW FV atmospheric module calculates the transfer of mass/heat/momentum between the water column and the atmosphere.

4.8 Timestep Algorithm

The timestep algorithm within TUFLOW FV is summarised in the following flowchart.

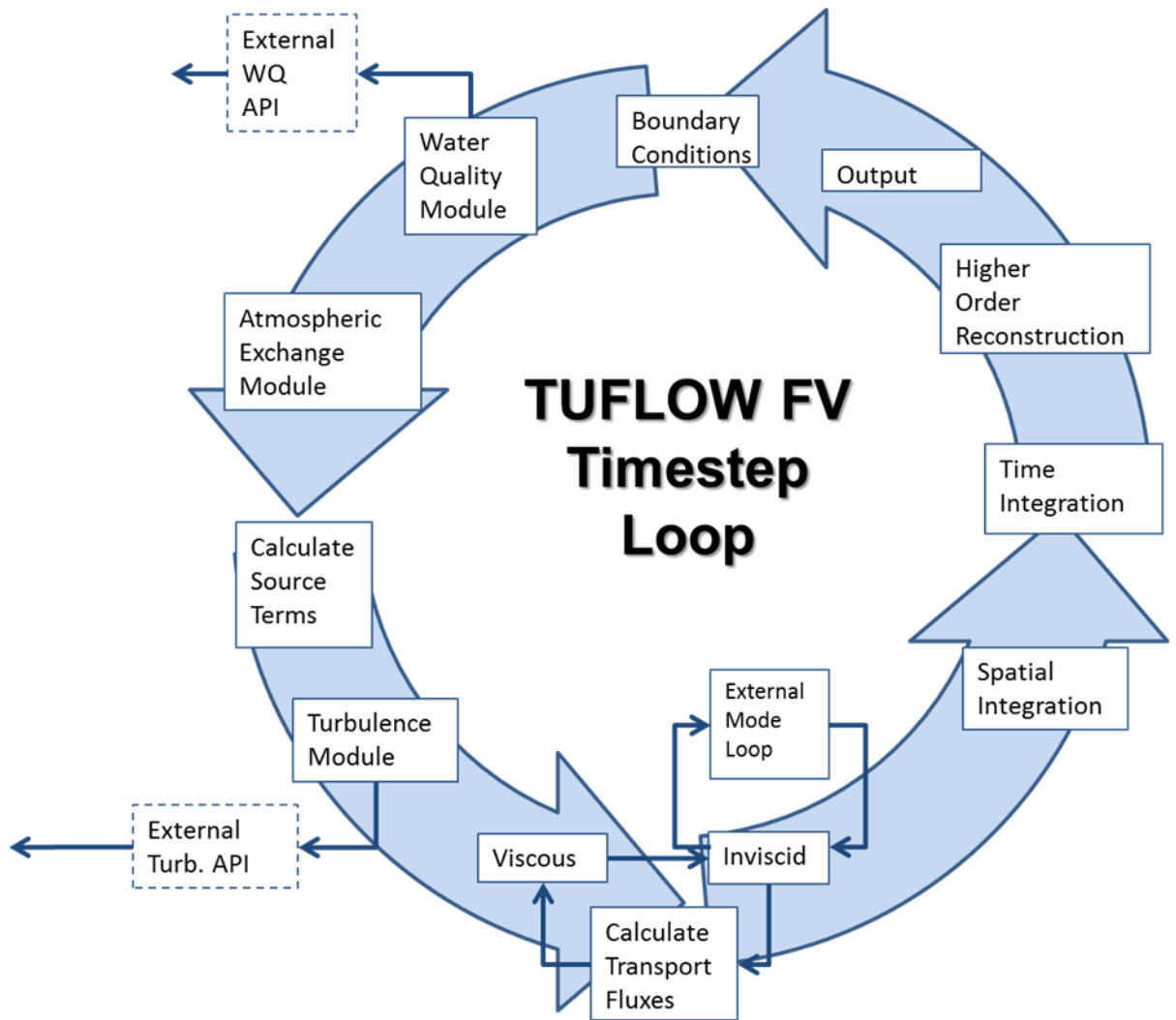


Figure 4-1 TUFLOW FV timestep loop illustration (further details outlined in Table 2)

Table 4-2 TUFLOW FV timestep algorithm

Update Fields	
<ul style="list-style-type: none"> • Write output • Update Boundary Condition data • Do Water Quality calculations • Do Sediment Transport calculations • Do atmospheric exchange calculations • Reset source terms • Update cell-centred boundary conditions • Update structure flows • Calculate horizontal and vertical turbulent viscosities & diffusivities • Calculate density • Calculate cell-face pressure differences (due to MSLP and baroclinic gradients) • Calculate internal mode inviscid fluxes • Calculate viscous fluxes • Calculate cell-centred source terms • Determine internal mode timestep 	
Enter external mode loop, initialising external mode variables	
	<ul style="list-style-type: none"> • Calculate external inviscid flux • Determine external mode timestep • Integrate the external inviscid flux wrt time • Calculate total external mode • Spatially integrate external mode fluxes • Perform conservative mass redistribution • Perform time integration • Update external mode sub-timestep • Apply ghost-cell boundary conditions • Calculate primitive variables • Update nodal values • Calculate face-centred gradients • Higher order scheme reconstruction (if required) • Update cell-face values • Update wet/dry flags
Exit external mode loop and perform internal mode flux corrections	
<ul style="list-style-type: none"> • Calculate horizontal scalar inviscid fluxes • Calculate total horizontal fluxes • Spatially integrate horizontal fluxes • Calculate depth change (time integrate depth-averaged continuity equation) • Calculate vertical fluxes (inviscid and viscous) • Perform time integration • Update timestep • Apply ghost-cell boundary conditions • Calculate primitive variables • Update nodal values • Calculate face-centred gradients • Higher order scheme reconstruction (if required) • Update cell-face values • Update wet/dry flags • Check model bounds 	

5 Atmospheric Exchange

TUFLOW FV offers a range of options for specifying and calculating atmospheric heat exchange, and thus water temperature. These options are described in the [TUFLOW FV User Manual](#). The associated underlying equations are presented here, in a manner that is aligned with the arrangement of content in User Manual. The supporting conceptual diagram of relevant radiation fluxes presented in the User Manual is repeated below for convenience.

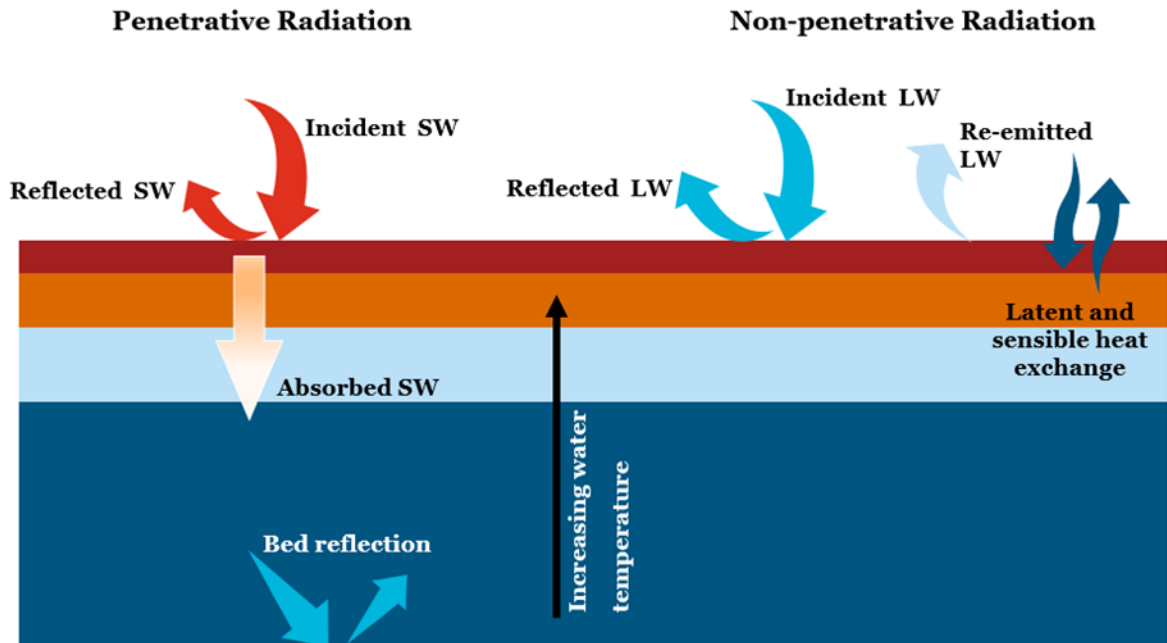


Figure 4-2 Atmospheric Heat Exchange Conceptual Diagram

TUFLOW FV's treatment of radiation fluxes under ice cover is not presented here. Contact support@tufLOW.com for further information.

5.1 Shortwave Radiation

The shortwave radiation models presented in Table 5-1 are available in TUFLOW FV.

Table 5-1 Shortwave Radiation Models

Method	Details	Required Data Inputs
{1} Default	Incident short wave radiation estimated according to Jacquet (1983).	Downward shortwave radiation (W/m ²). Positive is downwards.
2	Incident short wave radiation under clear sky estimated according to Zillman (1972) with cloud cover correction factor given by Reed (1977).	Air temperature (degrees C), relative humidity (%) and optionally cloud cover (decimal fraction between 0.0 and 1.0). If cloud cover is not specified a clear sky is assumed. Positive is downwards.

5.1.1 Shortwave Radiation Model 1

Incident shortwave radiation is estimated according to Jacquet (1983) as follows.

1. Compute albedo

$$\alpha_{\phi} = \alpha + 0.02 \sin\left(\frac{2\pi \times \text{day}}{365} \pm \frac{\pi}{2}\right) \quad (32)$$

where:

- α_{ϕ} [-] is the albedo corrected for latitude
- α [-] is the user specified (or default) albedo without latitudinal correction
- day [-] is the day of year
- \pm is positive and negative for northern and southern latitudes, respectively

2. Compute incident shortwave radiation

$$SW_i = (1.0 - \alpha_{\phi}) \times SW \times SS \quad (33)$$

where:

- SW_i [W/m²] is the surface shortwave radiation corrected for albedo and applied to the water surface
- α_{ϕ} [-] is the albedo corrected for latitude
- SW [W/m²] is the user specified incoming shortwave radiation
- SS [-] is the user specified solar shading coefficient (WQ Module only)

5.1.2 Shortwave Radiation Model 2

Incident shortwave radiation is estimated according to Zillman (1972) and Reed (1977) as follows.

1. Compute solar beam irradiance S_e [W/m^2] based on month (where day is day of year, corrected for leap years as required)

$$S_e = -0.2 \times (\text{day} - 1) + 1426 \quad \text{January (34)}$$

$$S_e = -\frac{17}{27} \times (\text{day} - 1) + 1420 \quad \text{February (35)}$$

$$S_e = -\frac{23}{30} \times (\text{day} - 1) + 1403 \quad \text{March (36)}$$

$$S_e = -\frac{23}{30} \times (\text{day} - 1) + 1380 \quad \text{April (37)}$$

$$S_e = -\frac{20}{30} \times (\text{day} - 1) + 1360 \quad \text{May (38)}$$

$$S_e = -\frac{5}{29} \times (\text{day} - 1) + 1340 \quad \text{June (39)}$$

$$S_e = -\frac{5}{30} \times (\text{day} - 1) + 1335 \quad \text{July (40)}$$

$$S_e = 1380 \quad \text{August (41)}$$

$$S_e = 1380 \quad \text{September (42)}$$

$$S_e = -\frac{22}{30} \times (\text{day} - 1) + 1380 \quad \text{October (43)}$$

$$S_e = -\frac{20}{29} \times (\text{day} - 1) + 1400 \quad \text{November (44)}$$

$$S_e = -\frac{6}{30} \times (\text{day} - 1) + 1420 \quad \text{December (45)}$$

2. Compute declination

$$h = \frac{180}{\pi} \arcsin \left(\sin \left(\frac{\text{lat} \times \pi}{180} \right) \times \sin \Delta + \cos \left(\frac{\text{lat} \times \pi}{180} \right) \times \cos \Delta \times \cos \pi \left(\frac{\text{time} - 12}{12} \right) \right) \quad (46)$$

where:

- h [degrees] is the declination
- lat [-] is latitude
- time [hours] is time of day

and:

$$\Delta = 6.918 \times 10^{-3} + 0.0257 \sin(\beta) - 3.99912 \times 10^{-1} \cos(\beta) + 9.07 \times 10^{-4} \sin(2\beta) - 6.758 \times 10^{-3} \cos(2\beta) - 1.48 \times 10^{-3} \times \sin(3\beta) - 2.697 \times 10^{-3} \cos(3\beta) \quad (47)$$

and:

$$\beta = \frac{2\pi \times \text{day}}{\text{year}} \quad (48)$$

where:

- day [-] is the day of year
- year [-] is the number of days in the year, which is either 365 or 366

3. Compute clear sky shortwave radiation without latitudinal correction

$$SW_{cs} = \frac{S_e \times \Gamma^2}{((\Gamma + 2.7) \times 10^{-5} \times P + 1.085 \times \Gamma + 0.1)} \quad (49)$$

where:

- SW_{cs} [W/m²] is the clear sky shortwave radiation without latitudinal correction
- S_e [W/m²] is the solar beam irradiance computed as above
- Γ [-] is

$$\left(\sin\left(\frac{\text{lat} \times \pi}{180}\right) \times \sin \Delta + \cos\left(\frac{\text{lat} \times \pi}{180}\right) \times \cos \Delta \times \cos \pi \left(\frac{\text{time} - 12}{12}\right) \right) \quad (50)$$

- P [Pa] is the vapour pressure:

$$P = \frac{RH}{100} \times SVP \quad (51)$$

and:

- RH [%] is the user specified relative humidity
- SVP [Pa] is the standard vapour pressure:

$$SVP = 100 \times e^{\left(2.3026 \times \left(\frac{7.5T}{T+237.3} + 0.758\right)\right)} \quad (52)$$

- T [C] is air temperature

4. Compute cloud cover correction if more than 25% cloud cover is present

$$SW_{cc} = SW_{cs} \times (1 - 0.62CC + 1.9 \times 10^{-3}H_n) \quad (53)$$

where:

- SW_{cc} [W/m²] is the cloudy sky shortwave radiation without latitudinal correction
- SW_{cs} [W/m²] is the clear sky shortwave radiation without latitudinal correction
- CC [-] is the user defined fractional cloud cover
- H_n [-] is:

$$\left(\sin\left(\frac{\text{lat} \times \pi}{180}\right) \times \sin \Delta + \cos\left(\frac{\text{lat} \times \pi}{180}\right) \times \cos \Delta \right) \quad (54)$$

- SW_{cc} [W/m²] is set to be equal to SW_{cs} if less than 25% cloud cover is present

5. Look up albedo α_ϕ from Zillman (1972) table using cloud cover (converted to octants by TUFLOW FV) and declination h computed above.
6. Compute incident shortwave radiation

$$SW_i = (1.0 - \alpha_\phi) \times SW_{cc} \times SS \quad (55)$$

where:

- SW_i [W/m²] is the surface shortwave radiation corrected for albedo and latitude and applied to the water surface
- α_ϕ [-] is the albedo from Zillman (1972) as above
- SW_{cc} [W/m²] is the computed incoming shortwave radiation allowing for cloud cover computed as above
- SS [-] is the user specified solar shading coefficient (WQ Module only)

5.2 Longwave Radiation

The longwave radiation models presented in Table 5-2 are available in TUFLOW FV. The intention for all models is to compute net longwave radiation.

Table 5-2 Longwave Radiation Models

Method	Details	Required Data Inputs
1	Net longwave radiation (accounting for both the incident long wave radiation and long wave radiation emitted at the water surface).	Net downward longwave radiation (W/m ²). Positive is downwards.
{2} Default	Incident longwave radiation is specified. Reflection is computed using an albedo, and longwave radiation emitted by the water surface is calculated assuming the Stefan-Boltzmann law.	Incident downward longwave radiation (W/m ²). Positive is downwards.
3	Incident longwave radiation (generated by air) is calculated assuming the Stefan-Boltzmann law with a correction for cloud cover following TVA (1972). The method includes water surface reflection of longwave radiation based on an albedo.	Air temperature (°C) and cloud cover.
4	Incident longwave radiation (generated by air) is calculated assuming the Stefan-Boltzmann law with a latitudinal correction for cloud cover. The method includes water surface reflection of longwave radiation based on an albedo. The long wave radiation emitted by the water surface is computed using the air/water temperature difference following Zillman (1972). This uses a similar method to Model 3 but uses a mix of air and water temperatures for this calculation.	Air temperature (°C) and cloud cover.
5	Incident longwave radiation (generated by air) is calculated based on air temperature and vapour pressure (Chapra, 2008). Reflectivity and generation of longwave by water are also included.	Air temperature (°C) and relative humidity (%).

5.2.1 Longwave Radiation Model 1

Net longwave radiation is provided by the user. No calculations are required.

5.2.2 Longwave Radiation Model 2

Net longwave radiation is computed as follows.

1. Compute incident longwave radiation

$$LW_i = LW \times (1 - \alpha)$$

(56)

where:

- LW_i [W/m²] is the incident longwave radiation corrected for albedo
- LW [W/m²] is the user specified incoming longwave radiation
- α [-] is the longwave radiation albedo

2. Compute outgoing longwave radiation emitted at the water surface

$$LW_o = \epsilon_w \times \sigma \times (T_w + 273.15)^4 \quad (57)$$

where:

- LW_o [W/m²] is the outgoing longwave radiation emitted at the water surface
- ϵ_w [-] is the emissivity of water
- σ [K W/m²] is the Stefan-Boltzmann constant (= 5.6704×10⁻⁸)
- T_w [C] is surface water temperature

3. Compute net longwave radiation

$$LW_{net} = LW_i - LW_o \quad (58)$$

where:

- LW_{net} [W/m²] is the net longwave radiation
- LW_i [W/m²] is the incoming longwave radiation
- LW_o [W/m²] is the outgoing longwave radiation emitted at the water surface

5.2.3 Longwave Radiation Model 3

Net longwave radiation is computed as follows.

1. Compute incident longwave radiation

$$LW_i = (1 - \alpha) \times (1 + 0.17CC^2) \times C_e \times (T_a + 273.15)^2 \times \sigma \times (T_a + 273.15)^4 \quad (59)$$

where:

- LW_i [W/m²] is the incident longwave radiation corrected for albedo
- α [-] is the longwave radiation albedo
- CC [-] is the user defined fractional cloud cover
- C_e [-] is the longwave constant for cloud cover (= 9.37×10⁻⁶)
- T_a [C] is the ambient air temperature
- σ [K W/m²] is the Stefan-Boltzmann constant (= 5.6704×10⁻⁸)

2. Compute outgoing longwave radiation emitted at the water surface

$$LW_o = \epsilon_w \times \sigma \times (T_w + 273.15)^4 \quad (60)$$

where:

- LW_o [W/m²] is the outgoing longwave radiation emitted at the water surface
- ϵ_w [-] is the emissivity of water
- σ [K W/m²] is the Stefan-Boltzmann constant (= 5.6704×10⁻⁸)
- T_w [C] is surface water temperature

3. Compute net longwave radiation

$$LW_{net} = LW_i - LW_o \quad (61)$$

where:

- LW_{net} [W/m²] is the net longwave radiation
- LW_i [W/m²] is the incoming longwave radiation
- LW_o [W/m²] is the outgoing longwave radiation emitted at the water surface

5.2.4 Longwave Radiation Model 4

Net longwave radiation is computed as follows.

1. Compute incident longwave radiation

$$LW_i = \sigma(1 - \alpha) \times (T_a + 273.15)^4 \times (0.92 \times 10^{-5}(T_a + 273.15)^2 - 1) \quad (62)$$

where:

- LW_i [W/m²] is the incident longwave radiation corrected for albedo
- σ [K W/m²] is the Stefan-Boltzmann constant (= 5.6704×10⁻⁸)
- α [-] is the longwave radiation albedo
- T_a [C] is the ambient air temperature

2. Compute outgoing longwave radiation

$$LW_o = 4(1 - \alpha) \times \sigma(T_a + 273.15)^3 \times (T_w - T_a) \quad (63)$$

where:

- LW_o [W/m²] is the outgoing longwave radiation emitted at the water surface
- α [-] is the longwave radiation albedo
- σ [K W/m²] is the Stefan-Boltzmann constant (= 5.6704×10⁻⁸)
- T_a [C] is the ambient air temperature
- T_w [C] is surface water temperature

3. Compute net longwave radiation

$$LW_{net} = (1 - 0.63CC) \times (LW_i - LW_o) \quad (64)$$

where:

- LW_{net} [W/m²] is the net longwave radiation
- CC [-] is the user defined fractional cloud cover
- LW_i [W/m²] is the incoming longwave radiation
- LW_o [W/m²] is the outgoing longwave radiation emitted at the water surface

5.2.5 Longwave Radiation Model 5

Net longwave radiation is computed as follows.

1. Compute incident longwave radiation

$$LW_i = \sigma(1 - \alpha) \times (T_a + 273.15)^4 \times \left(0.6 + 0.031 \sqrt{\frac{4.596RH}{100} e^{\frac{17.27T_a}{T_a + 273.15}}} \right) \quad (65)$$

where:

- LW_i [W/m²] is the incident longwave radiation corrected for albedo
- σ [K W/m²] is the Stefan-Boltzmann constant (= 5.6704×10⁻⁸)
- α [-] is the longwave radiation albedo
- T_a [C] is the ambient air temperature
- RH [%] is the ambient relative humidity

2. Compute outgoing longwave radiation

$$LW_o = \epsilon_w \times \sigma \times (T_w + 273.15)^4 \quad (66)$$

where:

- LW_o [W/m²] is the outgoing longwave radiation emitted at the water surface
- ϵ_w [-] is the emissivity of water
- σ [K W/m²] is the Stefan-Boltzmann constant (= 5.6704×10⁻⁸)
- T_w [C] is surface water temperature

3. Compute net longwave radiation

$$LW_{net} = LW_i - LW_o \quad (67)$$

where:

- LW_{net} [W/m²] is the net longwave radiation
- LW_i [W/m²] is the incoming longwave radiation

- LW_o [W/m²] is the outgoing longwave radiation emitted at the water surface

5.3 Latent Heat Flux

Latent heat flux calculations are performed following computation of the above short- and longwave radiation fields. Regardless of which models are chosen to do so (these are described in the following sections) all compute the following, in order:

1. Vapour pressures
2. Specific humidities
3. Wind transfer coefficients
4. Latent heat flux

The following content is therefore sectioned accordingly.

Vapour pressures and specific humidities are both computed by only one of two independent methods (i.e. each method computes both 1. and 2. above and only one method can be selected to do both). These methods are therefore presented together within Section 5.3.1. for each method. Any method presented in Section 5.3.1.1 can be selected to compute wind transfer coefficients. The final calculation of latent heat flux has only one method, and this is presented in Section 5.3.1.2.

5.3.1 Vapour Pressures and Specific Humidities

The vapour pressure and specific humidity models presented in Table 5-3 are available in TUFLOW FV. The details of each model are described following.

Table 5-3 Vapour Pressure and Specific Humidity Models

Method	Details	Required Data Inputs
{1} Default	Vapour pressure is calculated by the Magnus-Tetens formula (TVA, 1972).	Air temperature (°C) and relative humidity (%) and wind speed (m/s).
2	Vapour pressure is calculated via modified equations based on Lowe (1977) and Reed (1977).	Air temperature (°C) and relative humidity (%) and wind speed (m/s).

5.3.1.1 Latent Heat Flux Model 1

Vapour pressures

Air and water vapour pressures are computed as follows.

1. Compute saturated vapour pressure of water in atmospheric air

$$P_{as} = 100 \times e^{2.3026 \left(7.5 \frac{T_a}{(T_a + 237.3)} + 0.7858 \right)} \quad (68)$$

where:

- P_{as} [Pa] is the saturated vapour pressure of water in atmospheric air
- T_a [C] is the ambient air temperature

2. Compute vapour pressure of water in atmospheric air

$$P_a = \frac{RH}{100} P_{as} \quad (69)$$

where:

- P_a [Pa] is the vapour pressure of water in atmospheric air
- RH [%] is the atmospheric relative humidity

3. Compute vapour pressure of water due to the presence of surface water

$$P_w = 100 \times e^{2.3026 \left(7.5 \frac{T_w}{(T_w + 237.3)} + 0.7858 \right)} \quad (70)$$

where:

- P_w [Pa] is the vapour pressure of water due to the presence of surface water
- T_w [C] is the surface water temperature

Specific Humidities

1. Compute the corresponding specific humidity of atmospheric air as

$$E_a = 0.622 \frac{P_a}{P} \quad (71)$$

where:

- E_a [-] is the specific humidity of atmospheric air
- P_a [Pa] is the vapour pressure of water in atmospheric air
- P [Pa] is atmospheric pressure

2. Compute the corresponding specific humidity due to the presence of surface water

$$E_w = 0.622 \frac{P_w}{P} \quad (72)$$

where:

- E_w [-] is the specific humidity due to the presence of surface water
- P_w [Pa] is the vapour pressure of water due to the presence of surface water
- P [Pa] is atmospheric pressure

3. Compute salinity correction to specific humidity due to the presence of surface water as

$$E_w = E_w \times \max(1 - E_{sal}(1) \times S - E_{sal}(2) \times S^2, E_{sal}(3)) \quad (73)$$

where:

- E_w [-] is the specific humidity due to the presence of surface water
- $E_{sal}(1:3)$ [-] are user specified (or default) salinity parameters
- S [g/L] is surface water salinity

5.3.1.2 Latent Heat Flux Model 2

Vapour pressures

Air and water vapour pressures are computed as follows.

1. Compute vapour pressure and saturated vapour pressure of water in atmospheric air by using Newton-Raphson's Method to iterate on wet bulb temperature

- a. Assume a first guess for wet bulb temperature as

$$T_{wb} = 0.7T_a \quad (74)$$

where:

- T_{wb} [C] is the wet bulb temperature
- T_a [C] is the ambient air temperature

- b. Estimate saturated vapour pressure of water in atmospheric air as

$$P_{as} = T_{wb}(T_{wb}(T_{wb}(T_{wb}(T_{wb}(6.136821 \times 10^{-11}T_{wb} + 2.034081 \times 10^{-8}) + 3.03124 \times 10^{-6}) + 2.650648 \times 10^{-4}) + 1.428946 \times 10^{-2}) + 0.4436519) + 6.1078 \quad (75)$$

where:

- P_{as} [mbar] is the saturated vapour pressure of water in atmospheric air
- T_{wb} [C] is the wet bulb temperature

- c. Estimate the vapour pressure of water in atmospheric air as

$$P_a = P_{as} - \left(6.6 \times 10^{-4}(1 + 1.5 \times 10^{-3}T_{wb}) \times (T_a - T_{wb}) \times \frac{P}{100}\right) \quad (76)$$

where:

- P_a [mbar] is the vapour pressure of water in atmospheric air
- P_{as} [mbar] is the saturated vapour pressure of water in atmospheric air
- T_{wb} [C] is the wet bulb temperature
- T_a [C] is the ambient air temperature
- P [Pa] is atmospheric pressure

- d. Estimate the partial derivative of the saturated vapour pressure of water in atmospheric air with respect to wet bulb temperature as

$$\frac{\partial P_{as}}{\partial T_{wb}} = T_{wb}(T_{wb}(T_{wb}(6.0T_{wb} \times 6.136821 \times 10^{-11} + 5.0 \times 2.034081 \times 10^{-8}) + 4.0 \times 3.03124 \times 10^{-6}) + 3.0 \times 2.650648 \times 10^{-4}) + 2.0 \times 1.428946 \times 10^{-2}) + 1.0 \times 0.4436519 \quad (77)$$

where:

- $\frac{\partial P_{as}}{\partial T_{wb}}$ [mbar/C] is the partial derivative of the saturated vapour pressure of water in atmospheric air with respect to wet bulb temperature
- T_{wb} [C] is the wet bulb temperature

- e. Estimate partial derivative of the vapour pressure of water in atmospheric air with respect to wet bulb temperature as

$$\frac{\partial P_a}{\partial T_{wb}} = \frac{\partial P_{as}}{\partial T_{wb}} - \left(6.6 \times 10^{-4} (1.5 \times 10^{-3} T_a - 1.0 - 2.0 \times 1.5 \times 10^{-3} T_{wb}) \times \frac{P}{100} \right) \quad (78)$$

where:

- $\frac{\partial P_a}{\partial T_{wb}}$ [mbar/C] is the partial derivative of the vapour pressure of water in atmospheric air with respect to wet bulb temperature
- $\frac{\partial P_{as}}{\partial T_{wb}}$ [mbar/C] is the partial derivative of the saturated vapour pressure of water in atmospheric air with respect to wet bulb temperature
- T_a [C] is the ambient air temperature
- T_{wb} [C] is the wet bulb temperature
- P [Pa] is atmospheric pressure

- f. Calculate the next estimate of wet bulb temperature using the above computed quantities as

$$T_{wb} = T_{wb} - \frac{P_a - P_{as} \times \frac{RH}{100}}{\frac{\partial P_a}{\partial T_{wb}} - \frac{\partial P_{as}}{\partial T_{wb}} \times \frac{RH}{100}} \quad (79)$$

where:

- T_{wb} [C] is the wet bulb temperature
- P_a [mbar] is the vapour pressure of water in atmospheric air
- P_{as} [mbar] is the saturated vapour pressure of water in atmospheric air
- RH [%] is the ambient air relative humidity
- $\frac{\partial P_a}{\partial T_{wb}}$ [mbar/C] is the partial derivative of the vapour pressure of water in atmospheric air with respect to wet bulb temperature
- $\frac{\partial P_{as}}{\partial T_{wb}}$ [mbar/C] is the partial derivative of the saturated vapour pressure of water in atmospheric air with respect to wet bulb temperature

- g. Calculate the associated error using the computed quantities above as

$$E = \frac{\frac{P_a}{P_{as}} \frac{RH}{100}}{\frac{RH}{100}} \quad (80)$$

where:

- P_a [mbar] is the vapour pressure of water in atmospheric air
- P_{as} [mbar] is the saturated vapour pressure of water in atmospheric air
- RH [%] is the ambient air relative humidity

- h. Check error:

- If E is greater than 0.02 (i.e. a 2% difference) then repeat steps b to g above
- If E is less than or equal to 0.02 then finish iterating
- If E is still greater than 0.02 after 100 iterations, then use Method 1 as described in Section 5.3.1.1.

Specific Humidities

1. Compute the corresponding specific humidity of atmospheric air as

$$E_a = 0.622 \frac{P_a}{(P - 0.378P_a)} \quad (81)$$

where:

- E_a [-] is the specific humidity of atmospheric air
- P_a [Pa] is the vapour pressure of water in atmospheric air
- P [Pa] is atmospheric pressure

2. Compute the corresponding specific humidity due to the presence of surface water

$$E_w = 0.622 \frac{P_w}{P - 0.378P_w} \quad (82)$$

where:

- E_w [-] is the specific humidity due to the presence of surface water
- P_w [Pa] is the vapour pressure of water due to the presence of surface water
- P [Pa] is atmospheric pressure

3. Compute salinity correction to specific humidity due to the presence of surface water as

$$E_w = E_w \times \max(1 - E_{sal}(1) \times S - E_{sal}(2) \times S^2, E_{sal}(3)) \quad (83)$$

where:

- E_w [-] is the specific humidity due to the presence of surface water
- $E_{sal}(1:3)$ [-] are user specified (or default) salinity parameters

- S [g/L] is surface water salinity

5.3.2 Wind Transfer Coefficients

The wind transfer coefficient models presented in Table 5-4 are available in TUFLOW FV. These models do not depend on previous use of Latent Heat Flux Models 1 or 2 above.

Table 5-4 Wind Stress Models and Drag Coefficients

Wind Stress Model	Specification of Wind Drag Coefficient
1 (default)	If using the Wu Wind Stress Model the wind stress parameterisation is scaled based on wind speed using the Wind Stress Parameters command.
2	If using a Constant Wind Stress Model the wind stress parameterisation stays the same as pre-2019 builds and is applied using the Bulk Momentum Transfer Coefficient
3	If using Kondo Wind Stress Model it is possible to apply a scaling factor using a single term via the Wind Stress Parameters command. The effects of atmospheric stability on wind stress can be optionally included.

5.3.2.1 Wind Transfer Coefficient Model 1

The wind transfer coefficient is calculated as follows.

1. Set the density of air ρ_{air} [kg/m³] to the user defined (or default) value
2. Set the specific heat capacity of moist air $C_{p,\text{air}}$ [J/kg/m³] to the user defined (or default) value
3. Set the latent heat of vaporisation L_v [J/kg] as 2443300
4. Set the bulk aerodynamic latent heat transfer coefficient under neutral conditions Cl_n [-] as the user defined (or default) value
5. For user specified (or default) parameter values W_a [m/s], C_a [-], W_b [m/s] and C_b [-], compute wind transfer coefficient as

- a. If $W_{10_{\text{mag}}} < W_a$

$$C_{d10} = C_a \quad (84)$$

- b. Else, if $W_{10_{\text{mag}}} < W_b$

$$C_{d10} = C_a + (W_{10_{\text{mag}}} - W_a) \frac{C_b - C_a}{W_b - W_a} \quad (85)$$

- c. Else

$$C_{d10} = C_b \quad (86)$$

where:

- C_{d10} is the wind transfer coefficient
- $W10_{mag}$ [m/s] is the wind speed at 10 metres above the water surface

5.3.2.2 Wind Transfer Coefficient Model 2

The wind transfer coefficient is calculated as follows.

1. Set the density of air ρ_{air} [kg/m³] to the user defined (or default) value
2. Set the specific heat capacity of moist air $C_{p,air}$ [J/kg/m³] to the user defined (or default) value
3. Set the latent heat of vaporisation L_v [J/kg] as 2443300
4. Set the bulk aerodynamic latent heat transfer coefficient under neutral conditions Cl_n [-] as the user defined (or default) value
5. For user specified (or default) parameter values C_{dn} [-], compute wind transfer coefficient as

$$C_{d10} = C_{dn} \quad (87)$$

5.3.2.3 Wind Transfer Coefficient Model 3

1. Calculate the density of air as

$$\rho_{air} = \frac{3.4838 \times 10^{-3} P}{T_v + 273.15} \quad (88)$$

where:

- ρ_{air} [kg/m³] is the density of ambient air
- P [Pa] is atmospheric pressure
- T_v [C] is virtual temperature

where:

- $T_v = (T_a + 273.15) \times (1 + 0.608E_a) - 273.15$
- T_a [C] is the ambient air temperature
- E_a [-] is the specific humidity of atmospheric air computed previously

2. Calculate the specific heat of moist air as

$$C_{p,air} = 1.004(1 + 0.9E_a) \times 1000 \quad (89)$$

where:

- $C_{p,air}$ [J/kg/C] is the specific heat capacity of moist air
- E_a [-] is the specific humidity of atmospheric air computed previously

3. Calculate the latent heat of vaporisation as

$$L_v = 4.1868(597.31 - 0.56525T_a) \times 1000 \quad (90)$$

where:

- L_v [J/kg] is the latent heat of vaporisation
- T_a [C] is the ambient air temperature

4. Set the bulk aerodynamic latent heat transfer coefficient under neutral conditions Cl_n [-] as the user defined (or default) value

5. For user specified (or default) scale factor parameter F , compute wind transfer coefficient as

- a. If $W10_{mag} < 2.2\text{m/s}$

$$C_{d10} = F \frac{1.080(\max(0.3, W10_{mag})^{-0.150})}{1000} \quad (91)$$

- b. Elseif $2.2\text{m/s} \leq W10_{mag} < 5.0\text{m/s}$

$$C_{d10} = F \frac{0.771+0.0858W10_{mag}}{1000} \quad (92)$$

- c. Elseif $5.0\text{m/s} \leq W10_{mag} < 8.0\text{m/s}$

$$C_{d10} = F \frac{0.867+0.0667W10_{mag}}{1000} \quad (93)$$

- d. Elseif $8.0\text{m/s} \leq W10_{mag} < 25.0\text{m/s}$

$$C_{d10} = F \frac{1.200+0.0250W10_{mag}}{1000} \quad (94)$$

- e. Elseif $25.0\text{m/s} \leq W10_{mag}$

$$C_{d10} = F \frac{0.000+0.0730W10_{mag}}{1000} \quad (95)$$

where:

- C_{d10} is the wind transfer coefficient
- F is the user specified (or default) scale factor
- $W10_{mag}$ [m/s] is the wind speed at 10 metres above the water surface

This model also offers atmospheric stability calculations. Contact support@tufLOW.com for further information.

5.3.3 Latent Heat Flux Calculation

When the specific humidity due to the presence of surface water E_w [-] is greater than the specific humidity of atmospheric air E_a [-], calculate the latent heat flux as

$$Q_{lat} = Cl_n \times \rho_{air} \times L_v \times W10_{mag} \times (E_w - E_a) \quad (96)$$

where:

- Q_{lat} [J] is the latent heat flux
- Cl_n [-] is the bulk aerodynamic latent heat transfer coefficient under neutral conditions set previously
- ρ_{air} [kg/m³] is the density of ambient air set or computed previously
- L_v [J/kg] is the latent heat of vaporisation set or computed previously
- $W10_{mag}$ [m/s] is the wind speed at 10 metres above the water surface
- E_w [-] is the specific humidity due to the presence of surface water computed previously
- E_a [-] is the specific humidity of atmospheric air computed previously

5.4 Sensible Heat Flux Calculation

Sensible heat flux calculations are performed following latent heat calculations as

$$Q_{sen} = Cs_n \times Cp_{air} \times \rho_{air} \times W10_{mag} \times (T_a - T_w) \quad (97)$$

where:

- Q_{sen} [J] is the sensible heat flux
- Cs_n [-] is the user defined (or default) bulk aerodynamic sensible heat transfer coefficient under neutral conditions
- Cp_{air} [J/kg/C] is the specific heat capacity of moist air
- ρ_{air} [kg/m³] is the density of ambient air set or computed previously
- $W10_{mag}$ [m/s] is the wind speed at 10 metres above the water surface
- T_a [C] is the ambient air temperature
- T_w [C] is the surface water temperature

5.5 Total Heat Flux Calculation

Total heat flux following as

$$Q_{tot} = Q_{lat} + Q_{sen} + Q_{LW} \quad (98)$$

where:

- Q_{tot} [J] is the total net heat flux
- Q_{lat} [J] is the latent heat flux computed previously (Section 5.3)
- Q_{sen} [J] is the sensible heat flux computed previously (Section 5.4)
- Q_{LW} [J] is the longwave radiation heat flux computed previously (Section 5.2)

6 Benchmarking

A range of benchmark tests have been conducted to prove TUFLOW FV performance, including 2D and 3D tests. The following contains a selection of these tests; documentation of further tests can be provided upon request. Please contact support@tufLOW.com for more information.

6.1 Carrier et al. 2003 Initial Value Problem

In this problem an initial offshore water surface profile is specified (Figure 4-1) on a uniform 1:10 slope. The initial water velocity throughout the problem domain is zero. The initial-value-problem (IVP) technique introduced by Carrier, Wu and Yeh (2003) is used to produce the benchmark data. The benchmark task is to produce snapshots of the free surface and velocity profiles at $t = 160s$, $175s$, and $220s$. These comparisons are shown in Figure 4-2 and Figure . In addition, the trajectory of the shoreline is plotted in Figure 4. It is noted that the results from the TUFLOW FV model are in close agreement with the benchmark solution in all cases.

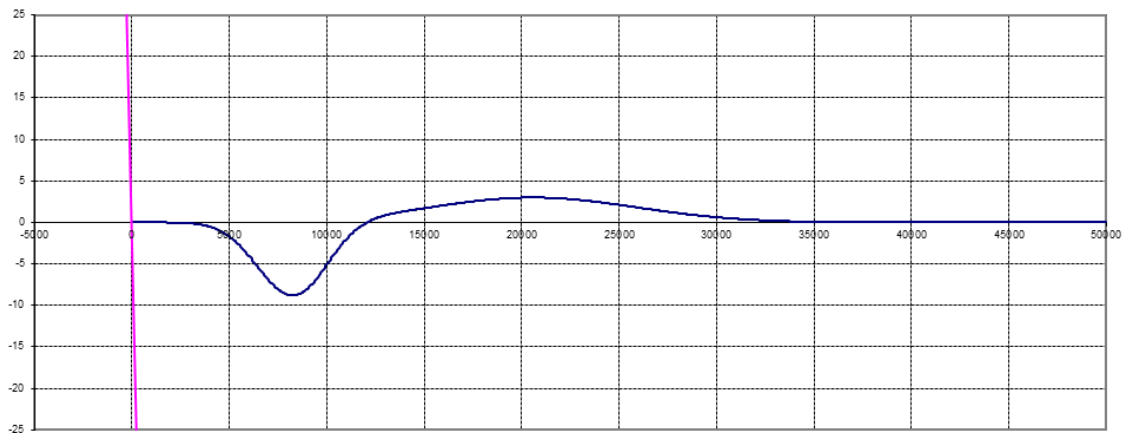
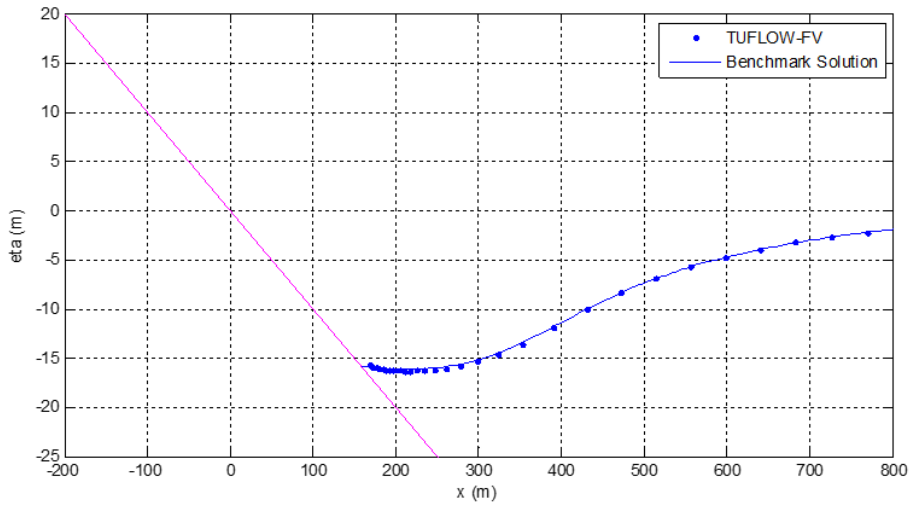
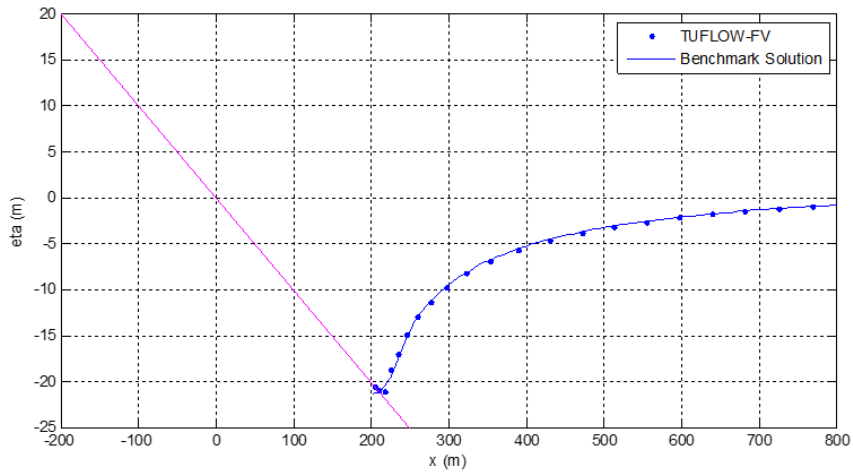


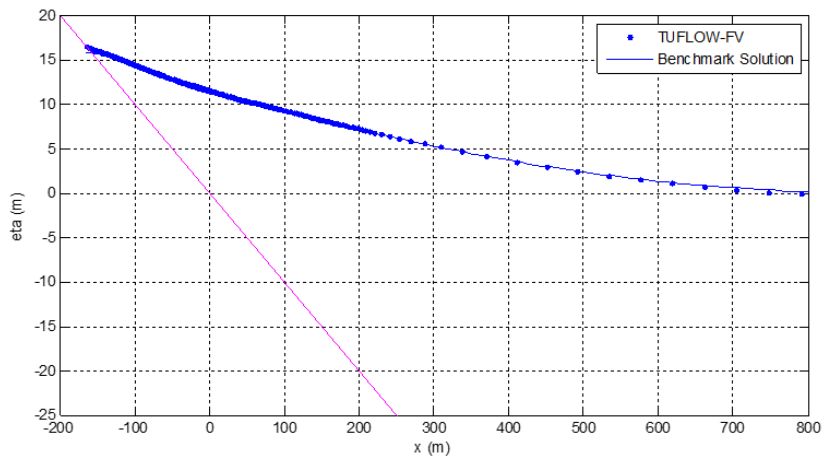
Figure 6-1 Initial water surface elevation plot at $t = 0s$



(a) $t = 160s$



(b) $t = 175s$



(c) $t = 220s$

Figure 6-2 Snapshots of water surface elevation at (a) 160s, (b) 175s and (c) 220s

6.2 Monai Valley, Okushiri Island

The 1993 Okushiri tsunami caused a runup of 32 m near the village of Monai in Okushiri Island. This tsunami runup mark was discovered at the tip of a very narrow gully within a small cove. This benchmark problem is a 1/400 scale laboratory experiment of the Monai runup, using a large-scale tank (205 m long, 6 m deep, 3.4 m wide) at Central Research Institute for Electric Power Industry (CRIEPI) in Abiko, Japan. The benchmark task is to reproduce the results of the laboratory experiment. Figure 6-3 shows the bathymetry and coastal topography used in the laboratory experiment, as well as the timeseries of water level prescribed at the offshore boundary. The other three boundaries are reflective sidewalls. The numerical model is required to reproduce the temporal and spatial variations of the shoreline location, as well as the temporal variations of the water-surface variations at three specified nearshore locations. Figures 6-4 and 6-5 illustrate the good performance of the model compared to the laboratory experimental results.

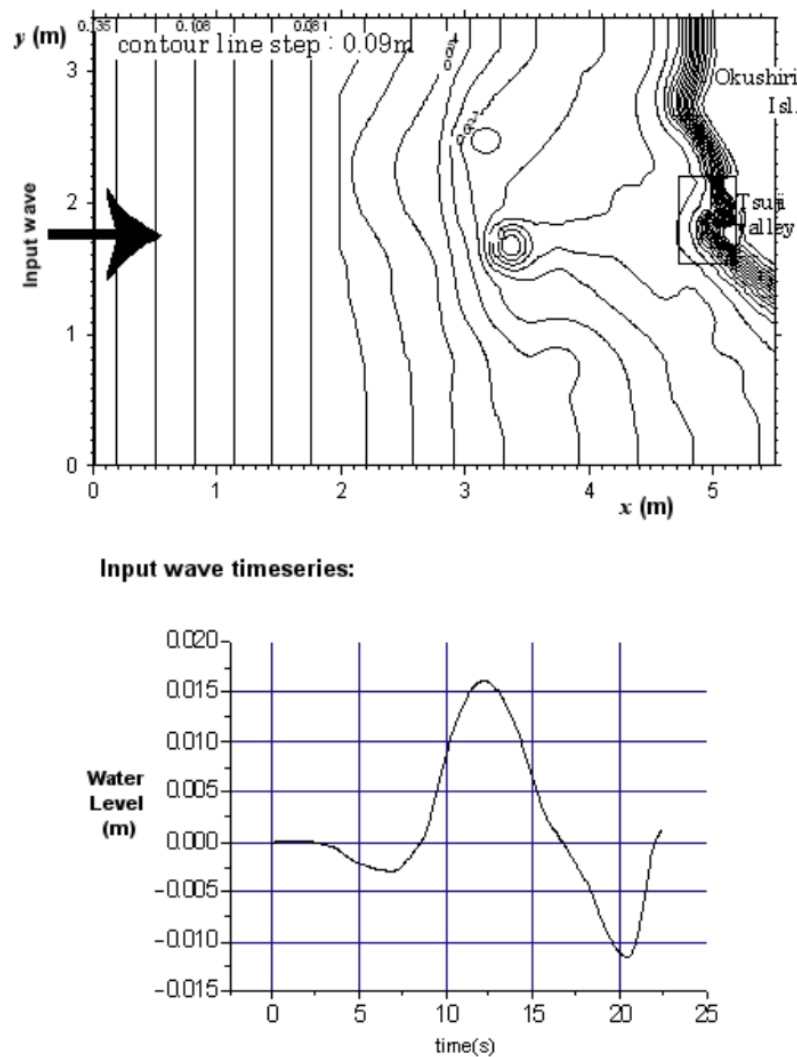


Figure 6-3 The laboratory experiment bathymetry and the water surface timeseries boundary condition

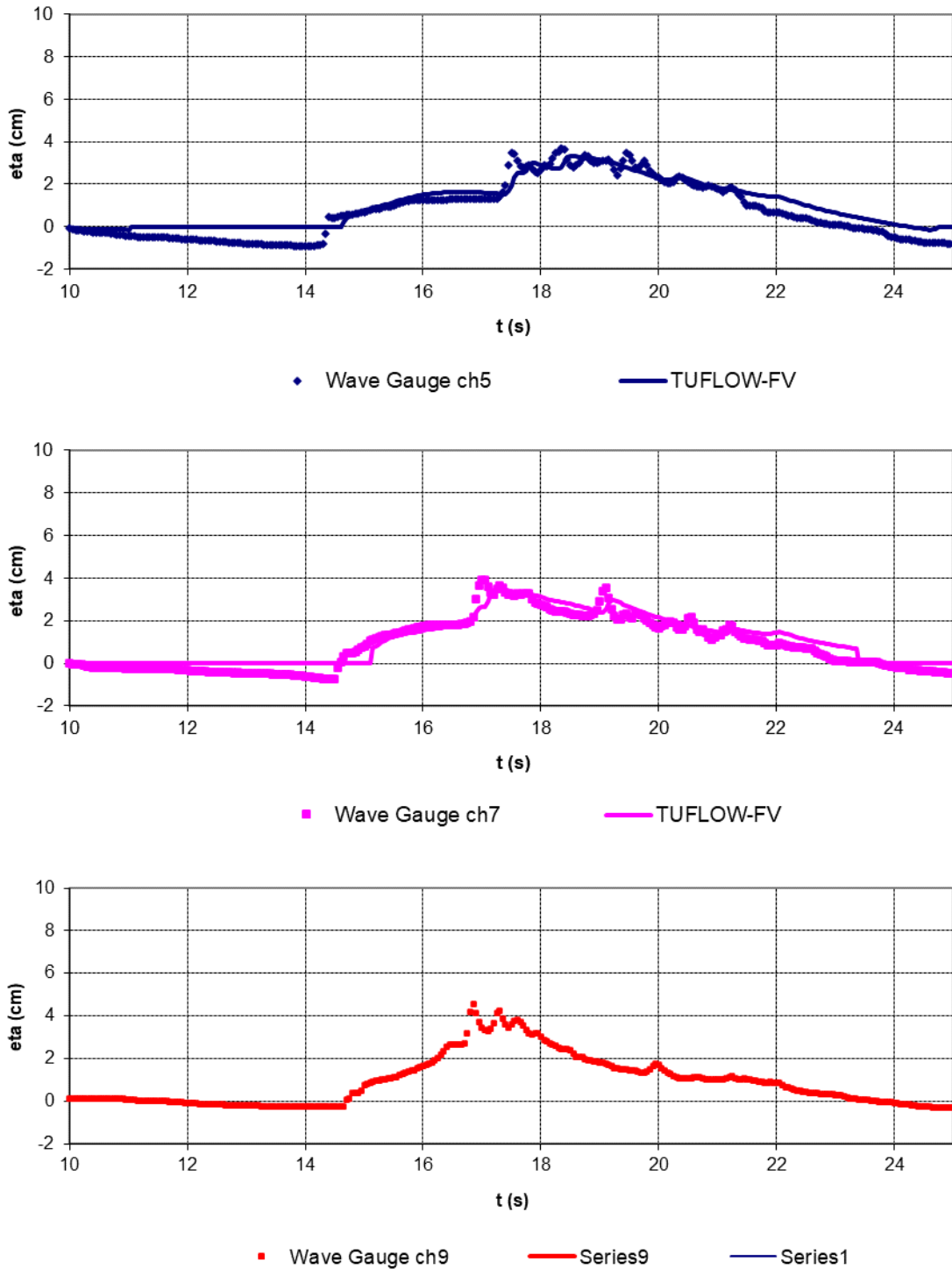


Figure 6-4 Timeseries of water surface elevation at wave gauges ch5, ch7 and ch9

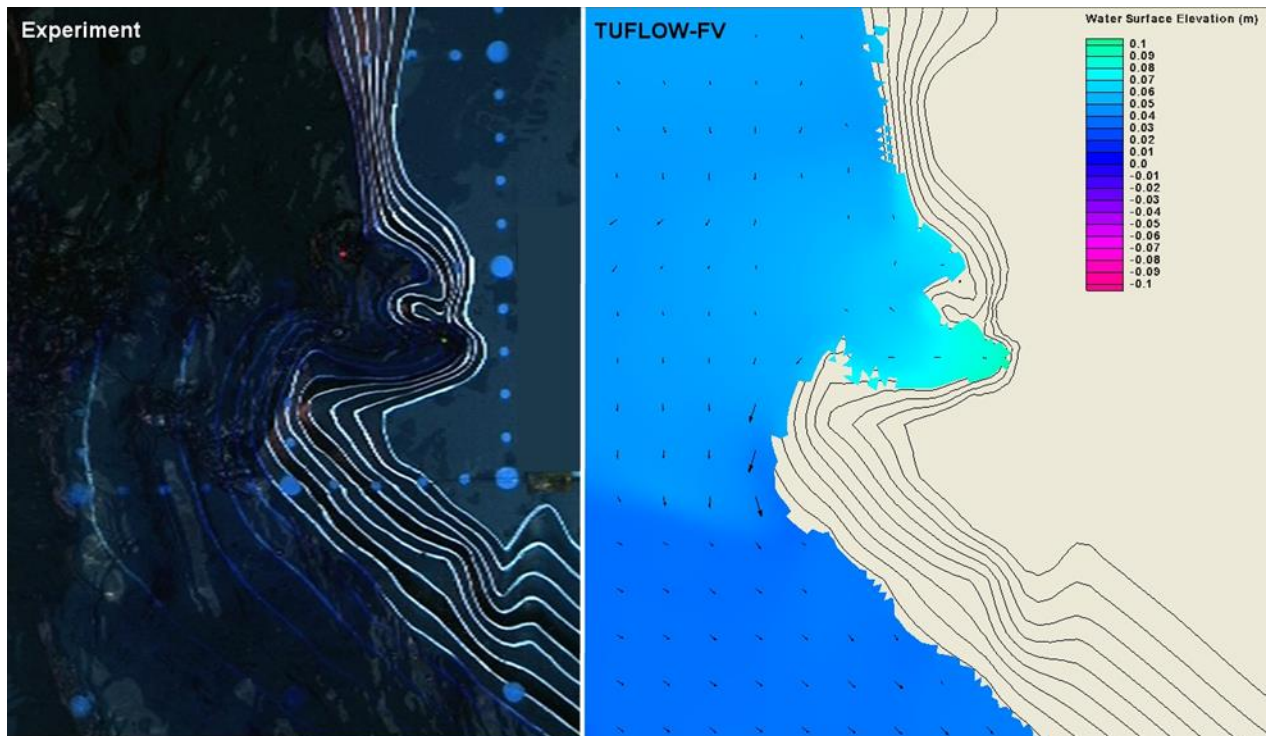


Figure 6-5 A snapshot of the modelled water surface at $t = 17.1s$ compared to a video snapshot from the laboratory experiment

6.3 UK Environment Agency Benchmarking Study

The “Desktop Review of 2D Hydraulic Modelling Packages” report (Néelz and Pender 2009) released in the United Kingdom by the Environment Agency highlighted the rapidly growing number of hydraulic modelling packages available for flood inundation estimation. A vast amount of documentation exists on appropriate applications of each modelling package however little of it discusses the influence that the choice of modelling package may have. The conclusions of the report recommended a series of benchmarking test cases to provide guidance on choosing the appropriate modelling package for future applications.

In response to the recommendations, a series of 10 2D flood inundation modelling benchmarking tests were conducted in 2010 using a variety of modelling packages. Additional testing was undertaken in 2012 and published in 2013 due to the availability of new modelling packages and the further development undertaken on existing modelling packages. 15 software development organisations tested a total of 19 modelling packages. The results are documented in the report, [“Benchmarking the Latest Generation of 2D Hydraulic Modelling Packages” \(Néelz, S. and Pender, G. 2013\)](#).

The TUFLOW suite was submitted for the initial phase of testing in 2010 with all three 2D schemes, TUFLOW’s implicit and explicit GPU solvers, and TUFLOW FV’s explicit solvers undergoing the more recent phase of testing in 2012. The results demonstrated consistency between each of the three TUFLOW engines and with other fully dynamic schemes. All three TUFLOW engines were found to be suitable for the following applications:

- Prediction of inundation extent;
- Prediction of maximum depth;
- Prediction of maximum velocity;
- Prediction of temporal variation in inundation extent;
- Prediction of temporal variation in depth; and
- Prediction of temporal variation in velocity.

The 10 tests are outlined in Table 6-1. For further information refer to [“Benchmarking the Latest Generation of 2D Hydraulic Modelling Packages” \(Néelz, S. and Pender, G. 2013\)](#).

All tests were completed using TUFLOW FV with the exception of Tests 7 and 8B. These two tests require 1D/2D linking which is currently in development.

Table 6-1 United Kingdom Environment Agency Benchmark Tests

Test Number	Description	Purpose
1	Flooding a disconnected water body	Assess basic capability to simulate flooding of disconnected water bodies on floodplains or coastal areas.
2	Filling of floodplain depressions	Tests capability to predict inundation extent and final flood depth for low momentum flow over complex topographies.
3	Momentum conservation over a small (0.25m) obstruction	Tests capability to simulate flow at relatively low depths over an obstruction with an adverse slope.
4	Speed of flood propagation over an extended floodplain	Tests simulation of speed of propagation of flood wave and the prediction of velocities at the leading edge of the advancing flood.
5	Valley flooding	Tests simulation of major flood inundation at the valley scale.
6A and 6B	Dam break	Tests simulation of shocks and wake zones close to a failing dam.
7	River to floodplain linking	Evaluates capability to simulate flood volume transfer between rivers and floodplains using 1D to 2D model linking. This test has not yet been undertaken for TUFLOW FV but will be included following 1D/2D integration.
8A and 8B	Rainfall and sewer surcharge flood in urban areas	Tests capability to simulate shallow flows in urban areas with inputs from rainfall (8A) and sewer surcharge (8B). Test 8B has not yet been undertaken for TUFLOW FV but will be included following 1D/2D integration.

7 References

- Batten, P. *et al.* (1996) 'Positively conservative high-resolution convection schemes for unstructured elements', *International journal for numerical methods in engineering*, 39, 1821-1838.
- Brufau, P. *et al.* (2004) 'Zero mass error using unsteady wetting–drying conditions in shallow flows over dry irregular topography', *International journal for numerical methods in fluids*, 45, 1047-1082.
- Chapra, S.C. (2008) *Surface water quality modelling*. Waveland Press
- Chow, V.T. (1959) *Open channel hydraulics* New York: MacGraw-Hill Book Company Incorporation
- Falconer, R.A. *et al.* (2005) 'Modelling water quality processes in estuaries', in Bates P.D, Lane S.N, Ferguson R.I. (ed.) *Computational fluid dynamics: applications in environmental hydraulics*. John Wiley & Sons.
- Fisher, H.B.(1979) *Mixing in inland and coastal waterways* Academic Press.
- Fringer, O.B. *et al.* (2005) 'Reducing numerical diffusion in interfacial gravity wave simulations' *International journal for numerical methods in fluids*, 49, 301-329.
- Hubbard, M.E. (1999) 'Multidimensional slope limiters for MUSCL-type finite volume schemes on unstructured grids', *Journal of computational physics*, 155, 54–74.
- Hubbard, M.E. *et al.* (2000) 'Flux difference splitting and the balancing of source terms and flux gradients' *Journal of computational physics*, 165, 89–125.
- Jacquet, J. (1983) *Simulation of the thermal regime of rivers* in Orlob, G.T (ed.) *Mathematical modeling of water quality: Streams lakes, and reservoirs* Wiley-Interscience, 150-176.
- Leveque, R.J. (2002) *Finite volume methods for hyperbolic problems* Cambridge University Press.
- Lowe, P.R. (1977) 'An approximating polynomial for the computation of saturation vapor pressure', *Journal of applied meteorology and climatology*, 16(1), 100-103.
- Munk, W.H. *et al.* (1948) 'Notes on the theory of the thermocline', *Journal of marine research*, 3, 276-295.
- Murillo, J. *et al.* (2005) 'Coupling between shallow water and solute flow equations: analysis and management of source terms in 2D' *International journal for numerical methods in fluids*, 49, 267-299.
- Murillo, J. *et al.* (2006) 'A conservative 2D model of inundation flow with solute transport over dry bed', *International journal for numerical methods in fluids*, 52, 1059–1092.
- Reed, R.K. (1997) 'On estimating insolation over the ocean', *Journal of physical oceanography*, 7(3), 482-485.
- Roe, P.L. (1981) 'Approximate Riemann solvers, parameter vectors and difference schemes', *Journal of computational physics*, 43, 357-372.
- Rossmannith, J.A. *et al.* (2004) 'A wave propagation algorithm for hyperbolic systems on curved manifolds' *Journal of computational physics*, 199, 631-662.
- Salhotra, A.M. *et al.* (1985) 'Effect of salinity and ionic composition on evaporation: analysis of Dead Sea evaporation pans', *Water Resources Research*, 21, 1336–1344.

Shchepetkin, A.F. *et al.* (2005) 'The regional oceanic modeling system (ROMS): a split-explicit, free-surface, topography-following-coordinate oceanic model', *Ocean Modelling*, 9 (4), 347-404.

Tennessee Valley Authority (TVA), (1972). Heat and mass transfer between a water surface and the atmosphere. Water Resources Research, Laboratory Report No. 14. Engineering Laboratory, Division of Water Control Planning, Tennessee Valley Authority, Norris Tennessee.

Wu, J. (1980) 'Wind-stress coefficients over sea surface and near neutral conditions – A revisit', *Journal of Physical Oceanography*, 10, 727-740.

Wu, J. (1982) 'Wind-stress coefficients over sea surface from breeze to hurricane', *Journal of Geophysical Research*, 87(C12), 9704-9706.

Zillman, J.W. (1972) 'A study of some aspects of the radiation and heat budgets of the southern hemisphere oceans', *Australian Government Publishing Service. Meteorological Study*, 26, 562